



Article

Identifying the Potential Dam Sites to Avert the Risk of Catastrophic Floods in the Jhelum Basin, Kashmir, NW Himalaya, India

Muzamil Ahmad Rather¹, Gowhar Meraj¹ , Majid Farooq¹, Bashir Ahmad Shiekh¹, Pankaj Kumar^{2,*} , Shruti Kanga³ , Suraj Kumar Singh⁴ , Netrananda Sahu⁵ and Surya Prakash Tiwari⁶

- ¹ Department of Ecology, Environment & Remote Sensing, Government of Jammu & Kashmir, SDA Colony Bemina, Srinagar 190018, India; rsmuzzammil@yahoo.com (M.A.R.); gowharmeraj@gmail.com (G.M.); majid_rsgis@yahoo.com (M.F.); geosbashir@gmail.com (B.A.S.)
- ² Institute for Global Environmental Strategies, Hayama 240-0115, Kanagawa, Japan
- ³ Centre for Climate Change, Suresh Gyan Vihar University, Jaipur 302017, India; shruti.kanga@mygyanvihar.com
- ⁴ Centre for Sustainable Development, Suresh Gyan Vihar University, Jaipur 302017, India; suraj.kumar@mygyanvihar.com
- ⁵ Department of Geography, Delhi School of Economics, University of Delhi, Delhi 110007, India; nsahu@geography.du.ac.in
- ⁶ Applied Research Center for Environment & Marine Studies, The Research Institute, King Fahd University of Petroleum & Minerals (KFUPM), Dhahran 31261, Saudi Arabia; surya.tiwari@kfupm.edu.sa
- * Correspondence: kumar@iges.or.jp



Citation: Rather, M.A.; Meraj, G.; Farooq, M.; Shiekh, B.A.; Kumar, P.; Kanga, S.; Singh, S.K.; Sahu, N.; Tiwari, S.P. Identifying the Potential Dam Sites to Avert the Risk of Catastrophic Floods in the Jhelum Basin, Kashmir, NW Himalaya, India. *Remote Sens.* **2022**, *14*, 1538. <https://doi.org/10.3390/rs14071538>

Academic Editor: Guy Schumann

Received: 3 February 2022

Accepted: 19 March 2022

Published: 22 March 2022

Publisher's Note: MDPI stays neutral with regard to jurisdictional claims in published maps and institutional affiliations.



Copyright: © 2022 by the authors. Licensee MDPI, Basel, Switzerland. This article is an open access article distributed under the terms and conditions of the Creative Commons Attribution (CC BY) license (<https://creativecommons.org/licenses/by/4.0/>).

Abstract: In September 2014, Kashmir witnessed a catastrophic flood resulting in a significant loss of lives and property. Such massive losses could have been avoided if any structural support such as dams were constructed in the Jhelum basin, which has a history of devastating floods. The GIS-based multicriteria analysis (MCA) model provided three suitability zones for dam locations. The final suitable dam sites were identified within the highest suitability zone based on topography (cross-sections), stream order, high suitable zone, minimum dam site interval, distance from roads, and protected area distance to the dam site. It was discovered that 10.98% of the total 4347.74 km² area evaluated falls in the high suitability zone, 28.88% of the area falls in the medium suitability zone, and 60.14% of the area falls in the low suitability zone. Within the study area, four viable reservoir sites with a holding capacity of 4,489,367.55 m³ were revealed.

Keywords: geospatial analysis; multicriteria analysis (MCA); site suitability; weighted overlay analysis; ALOS-PALSAR; Landsat OLI; flood management

1. Introduction

Floods are among the most dangerous natural hazards, resulting in property damage, devastation, human injuries, and death, particularly in the high alpine regions such as the Himalayas and the Alps [1–3]. These floods bring havoc to years of development, thus instantly draining governments' and people's resources [4,5]. Due to changes in climatic conditions and the resulting increase in variability of weather phenomena, there has been an increase in the number and intensity of flooding events in the alpine regions [6–8]. The adverse impact of the extreme flooding events on the people living in high alpine zones has also increased manifold, since last few decades due to population increase, urban sprawl, destruction of wetlands, and loss of natural vegetation [9–12].

In recent years, alpine regions have witnessed some of the century's worst floods. There have many notable flooding events in the Himalayas and the Alps; for example, on 3 August 2012, the Northern Himalayan states of India, parts of Uttarakhand, Himachal

Pradesh, Uttar Pradesh, and J&K witnessed heavy flash floods resulting in substantial loss of life and property [13]. On 7 February 2021, Chamoli, Uttarakhand, witnessed one of the worst floods in history, causing widespread damage to the life and property of the downstream populations [14]; similarly, there have also been similar incidences of flooding events in the Alps [15]. Recently, in July 2021, more than 120 people died due to one of the worst flooding in decades in the Western European countries coming under the catchment of the Alps [16]; such a situation is prevalent in almost every mountainous region of the World.

The present study has been carried out in one of the Himalayan regions of the World, the Jhelum basin (Kashmir valley), the catchment of one of the tributaries of the Indus water system i.e., the Jhelum river in India. With a history of hazardous events, it has seen a significant loss of life and property due to natural hazards such as earthquakes, landslides, and particularly floods [17,18]. The Jhelum basin has had over 25 severe flooding occurrences, with a mean expectation of 1 in every 4.3 years [19]. Experts owe this high frequency to the basic configuration of the Kashmir valley that renders it highly vulnerable to floods [20]. The oval shape of the valley surrounded by steep slope mountains, coupled with heavy rainfall of 2–3 days, can result in a severe flood disaster event [21].

In September 2014, the Jhelum basin witnessed 398 villages inundated and millions affected due to one of the worst floods in decades [22,23]. Many studies have been conducted since 2014 related to assessing the causes and consequences behind this event. Meraj et al. (2015) assessed the role of differential geoenvironmental settings of the Pir Panjal and Himalayan watersheds on the hydrological response at the basin floor [24], concluding that the Jhelum river's right and left-wing watershed streams drain water at different rates. Bhatt et al. (2017) conducted a detailed study of the causes and impacts of this flooding event. The study concluded that continuous heavy precipitation for several days (7 days) simultaneously over the entire basin resulted in the extreme flooding disaster of the region [21]. Romshoo et al. (2018) conducted a more detailed analysis of the 2014 flooding deluge in the Kashmir valley. The study ascribed causal effects of the flood to the intricate interaction of heavy rainfall, rugged geomorphic setup of the valley, anthropogenic factors, such as floodplain urbanization, decreased river channel capacity due to siltation, and the loss of wetlands; however, this study brought an important conclusion about the cause of this event, describing the south valley tributaries as having very high stream profile gradients, making them fast discharging watersheds with the least time of runoff concentration (minimal basin lag time) at their outlets. These watersheds during 2014-floods instantaneously released massive volumes of floodwaters into the Jhelum at the location called *Sangam* that resulted in an enormous surge of water, causing inundation of the basin floor from this location downstream due to a mild downstream gradient [25]. Meraj et al. (2018) conducted the hydrological characterization of the 24 watersheds of the Jhelum basin and concluded similarly that south valley watersheds have rapid hydrological responses. This study proposed a three-tier strategy for managing the floods in the Jhelum basin, i.e., prioritizing the watersheds based on their hydrological responses; finding out the locations for structural measures such as piano-key weirs and dam reservoirs; and an efficient disaster risk reduction policy [26].

Experts believe that dams could be one of the efficient mechanisms for delaying the hydrological response at critical locations such as at *Sangam* to avert the flooding downstream; moreover, it shall also help authorities to issue adequate early warning alerts. Globally, dams have been key in regulating the floods in the downstream locations [27], and several studies have been conducted to ascertain the effectiveness of dams in flood management. Mei et al. (2017) conducted research on 38 rivers in the United States to assess the impact of dams in reducing the flood magnitude at downstream locations. The study concluded that the magnitude of floods got substantially decreased in all the streams with dams [28]; almost similar results have been shown by studies conducted by Peyravi et al. (2018), Rokaya et al. (2019), Abbasi et al. (2019), Smys et al., 2020, Mohanty et al., 2020 and many others [29–32]. Besides efficiently managing floods downstream, dams are also useful

as water reservoirs for drinking, irrigation, sediment retention, and hydropower generation [33–36].

The increasing incidences of floods in the Jhelum basin are associated with the loss of lives and property over the last decade. To develop a concrete preventative management approach to save people's lives and property from the disastrous effects of floods, the establishment of several dams in the Jhelum basin is the need of the hour [27]. Selecting a dam location requires detailed studies on physiography, soil, the geology of the area, and the hydrology of the catchment. Globally, remote sensing and GIS-based methodologies are used to select the appropriate areas for selecting dams. These methods involve the selection of the relevant parameters and then using multicriteria-based decision-making (MCA) approach to arrive at the most suitable site (s) for the construction of the dam [37–39].

This work aims to locate potential dam sites in the Southern watersheds of Jhelum Basin, Jammu, and Kashmir, North-Western Himalaya of India, to avert the risk of catastrophic floods in the basin floor using a multicriteria analysis (MCA) based approach [40–44]. The Kashmir region lacks long-term hydrological data at a reasonable time scale for better flood forecasting and vulnerability assessment. In fact, this is the case with almost all the Himalayan regions, which is why the experts have been developing and using knowledge-based assessments of flood-related policy and decision-making strategies. This study's findings are part of a flood mitigation program of the Jhelum basin proposed to the Government of Jammu and Kashmir for innovative open-and-shut mechanism-based flood management during the storm events, leading to extreme flooding events.

2. Study Area

Jammu and Kashmir, India is located between $32^{\circ}16'48.475''$ to $34^{\circ}49'30.86''$ N latitude and $73^{\circ}44'58.126''$ to $76^{\circ}46'13.099''$ E longitude. The Kashmir valley (Jhelum basin) in Jammu and Kashmir has a well-established drainage system, with the Jhelum River serving as the primary drainage route. The Jhelum River (known as VYATH in Kashmir) has a spring source in the upper catchment area of the basin. The confluence of three streams, the Sandran, the Bringi, and the Aripath/Kuthar, transforms the Jhelum into a massive river [45]. The Jhelum basin comprises 24 tributaries, some of which flow from the slope of the Pir Panjal range and join the river on the left bank, while others flow from the Himalayan range and join the river on the right bank. The Jhelum River flows through the heart of Kashmir valley, between the Pir Panjal and Greater Himalayan mountain ranges (Zaskar Range) [46]. The Jhelum basin's geographical configuration makes it extremely vulnerable to natural disasters such as floods, earthquakes, landslides, and soil erosion; indeed, the area has been subjected to severe floods, resulting in loss of life and property. The Lidder, Kuthar, and Bringi watersheds from the Greater Himalayas (Zaskar range) and the Vishav, Rembiara, and Sandran watersheds from the Pirpanjal range were considered for study out of 24 catchments in the Jhelum basin. (Figure 1).

Temperature extremes mark the Kashmir valley because it is located in the continent's interior, far from the sea. July is the hottest month, with a mean temperature of 24.60°C , while January is the coldest, with a mean temperature of 10°C . Kashmir has a temperate climate with substantial seasonal variations. From November to March, the valley is blanketed in snow for five months of the year, when the average temperature in Srinagar is less than 10 degrees Celsius. Temperatures below 0 are ordinary in the winter, resulting in frost. From November to March, the valley floor receives most of its precipitation in the form of snow, while the mountain slopes receive it from October to the end of April. March, April, and May are the months with the most precipitation, while the mountains are still covered with snow till the end of June. This snow works as a water bank, maintaining the flow of water in the valley's streams, which is critical for irrigation. Only 20% of the total rainfall occurs in July and August due to the monsoons [47].

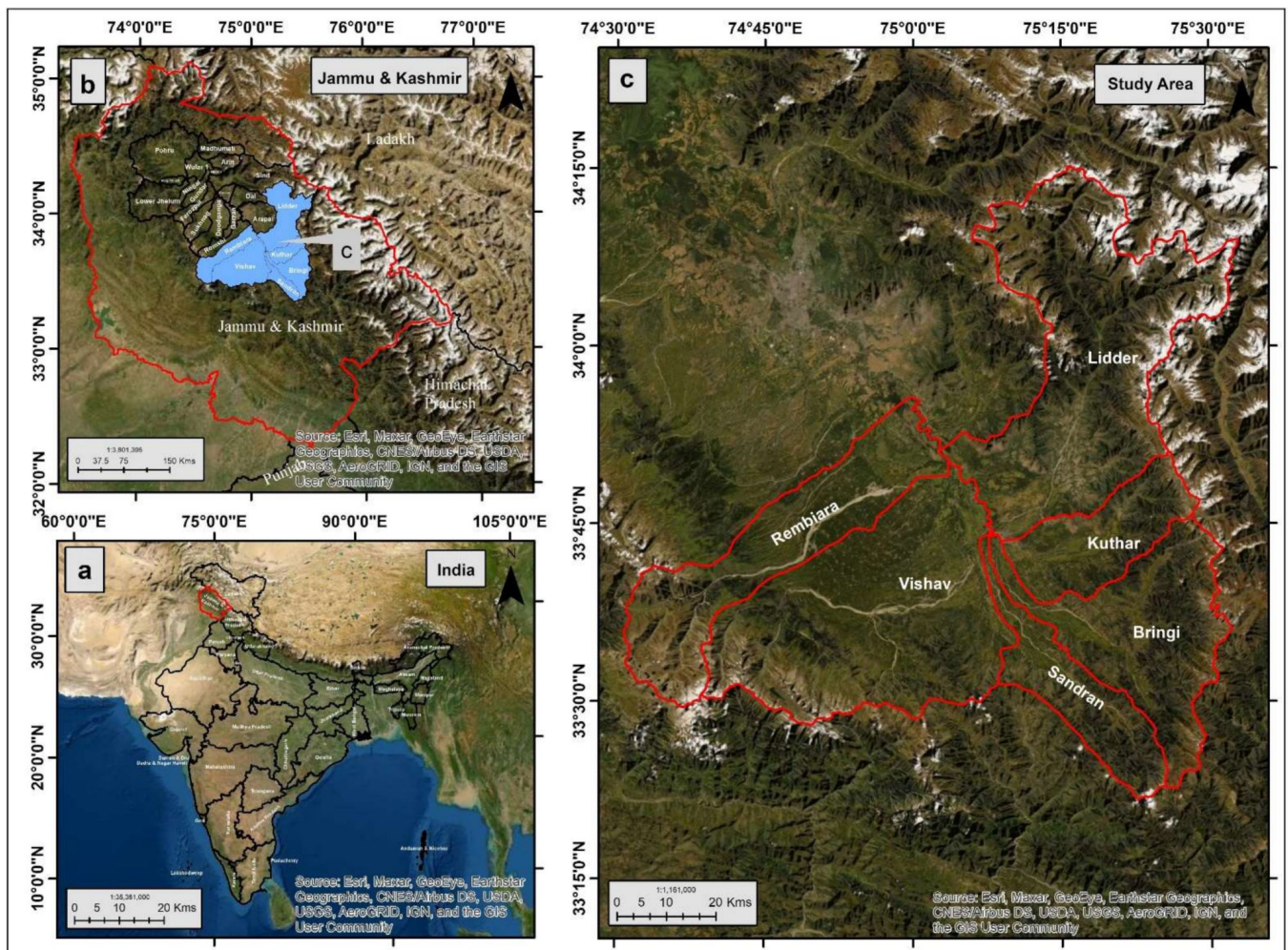


Figure 1. Location map: (a) The location of UT of Jammu, Kashmir, and Ladakh in relation to India (Red boundary); (b) The location of Kashmir valley, the western side of the UT; (c) The location of south Kashmir watersheds. The map coordinates are in the UTM 43 (North) World Geodetic System (WGS-1984) reference system.

3. Materials and Methods

3.1. Datasets

The various datasets used in the present study are shown in Table 1.

Table 1. Sources and information regarding the data used in the present study.

S. No	Data	Source	Details
1	Landsat 8 2018 Satellite Data	https://earthexplorer.usgs.gov/ (accessed on 31 February 2021)	30-m spatial resolution
2	ALOS-PALSAR DEM	Downloaded from Alaska Satellite Facility (ASF) Distributed Archive Center	12.5-m spatial resolution
3	Geological maps (1969)	Geological Survey of India	1:250,000
4	Soil maps	National Bureau of Soil Survey and Land Use Planning (NBSS&LUP)	1:500,000
5	Protected area (PA) Boundaries	Generated under the Protected Area Network Mapping Project	GPS-based field survey

3.2. Methods

3.2.1. Weighted Overlay Analysis

We used various information layers to find suitable areas for dam locations in the study area and included land use land cover (LULC), slope, elevation, geomorphology, lithology, lineament density, protected areas, CN grid, and soil.

LULC was obtained using the maximum likelihood classifier on Landsat-8, 2018 data [48]. The study area was divided into forest, scrub, pasture, farmland, built-up, barren rocky, and water classes. Accuracy assessment was conducted through comprehensive fieldwork using 278 field verification points using the Kappa coefficient [49].

$$k = \left\{ N \sum_{i=1}^r (X_{ii}) - N \sum_{i=1}^r (X_{i+} \cdot X_{+i}) \right\} / N^2 - \sum_{i=1}^r (X_{i+} \cdot X_{+i})$$

where,

r is the number of rows in the error matrix; X_{ii} denotes the number of observations in row i , and column i X_{i+} is the sum of the observations in row i . X_{+i} is the total number of observations in column i , and N is the total number of observations in the matrix.

For LULC classification, overall 93.52% of accuracy was achieved. The value of the kappa coefficient was 0.92 (Table 2).

Table 2. Accuracy assessment of LULC classification.

Class *	F	SH	PS	AC	AP	BU	WL	SG	W	Row Total	Accuracy
F	32				2					34	94.11
SH		40		4						44	90.90
PS			30							30	100.00
AC			4	28						32	87.50
AP	2				35					37	94.59
BU						40	3			43	93.02
WL						3	25			28	89.28
SG								10		10	100.00
W									20	20	100.00
Column Total	34	40	34	32	37	43	28	10	20	278	
Accuracy	94.11	100.00	88.23	87.50	94.59	93.02	89.28	100.00	100.00		

Overall accuracy $[(32 + 40 + 30 + 28 + 35 + 40 + 25 + 10 + 20)/278] \times 100 = 93.52\%$. * F Forest, SH Scrub, PS Pasture, AC Agriculture Cropland, AP Agriculture Plantation, BU Built-up, WL Wasteland, W waterbody, and SG Snow Glacial.

Topographical parameters, slope, elevation, drainage density were generated from ALOS-PALSAR DEM, which are important in deciding site suitability analysis for dams. DEM sinks were found and filled to ensure optimum flow direction and accumulation. A critical threshold of 200 m was used to generate drainage. Strahler's scheme of stream order was used for stream order classification [50].

Geological maps were used to generate geomorphology, lithology, and lineament layers using onscreen digitization. Lineament density raster was generated using the line density tool of Density Toolset of Spatial Analyst Toolbox. The geomorphology and lithology vector layers were converted to raster utilizing the feature to raster conversion tool in the ArcGIS 10.1. Similarly, soil maps were first digitized and then rasterized. Protected area (PA) boundaries used in the study in MCA were generated through a GPS-based field survey.

The curve number (CN) grid was also considered as one of the essential parameters for determining suitable dam sites in the multicriteria analysis framework. It was generated from LULC and hydrologic soil groups using the HEC-HMS model [51]. The DEM, the union of the soil group and land use, and the CN lookup table were used as inputs to generate the CN grid. A higher CN value indicates high runoff and low infiltration potential.

Finally, we resampled all the raster datasets to a standard cell size equivalent to the size of the ALOS-DEM (12.5 m) as most other layers were generated from DEM alone before overlay analysis. The weighted overlay analysis assigns weights to individual layers and scale values to the classes of those layers. This is a standard approach used in many studies involving MCA, and is referred to as knowledge-driven modeling [24]. Both scale and weightage were assigned after taking inputs from experts working in the field of hydrology and hydrogeology; moreover, since the number of classes varies in each thematic layer, the scale value could not be kept constant for all the layers. The variation in the scale value and the corresponding importance of various factors for dam site suitability was vetted by the collective judgment of the experts. Further, when many parameters are used in an MCA approach, some parameters tend to have more influence on the outputs than others. After we received the weightages and scale values for the parameters from experts, we performed the sensitivity analysis of these weights and scale values and tailored our final weights and scales accordingly. The weights and scales used in the study are the final values after sensitivity analysis results; however, it must be noted that the sensitivity imparted to parameters in the present case was only a function of the scale of the information layer and is not similar to the sensitivity of parameters in the physically-based mathematical models. Various researchers have used this method for the identification of dam sites, such as Refs. [43,52–54] (Figure 2).

Depending on the number of classes in a thematic layer, higher scale values were assigned to the pixels suitable for the dam site, and lower values were given to less suitable pixels. The relative importance of different layers and their weightages have been discussed in the results section. The weighted overlay analysis helped map highly suitable zones for dam construction, and the resultant map was referred to as a dam suitability map. The highest suitable zone was used for mapping the exact site location. The overall methodology used in this study to achieve the research objectives is outlined in Figure 2.

3.2.2. Determining the Dam Locations

Six criteria were chosen for deciding the exact locations for dam construction. Firstly, topography, where DEM and visual interpretation were used to analyze the locations' profile graphs (cross-sections). A good area for dam building is where a vast valley with high walls connects to a small canyon with sturdy walls [55]. Profile graphs (cross-sections) were created using interpolate line and profile graph tools of 3D Analyst Toolbox. Secondly, among the suitable zones identified in the final suitability map, a highly suitable zone is used to locate the final exact locations for dam construction. Thirdly, the fifth-order streams were used to locate the precise place of the dam building since the higher stream order is connected with more significant discharge available for a dam. The fourth criterion was the minimum dam site interval that ensures a good distribution of the dam sites. This way, water from different streams in different watersheds can be harnessed for storage and flood management purposes. An environmentally-friendly approach with a minimum distance (>6 km) between two dams was considered. The fifth one was the distance from roads to the dam site to minimize the cost of dam construction, and that distance between the nearest road and dam site was set to be less than 500 m. Finally, distance from protected areas to the dam site to conserve the rich biodiversity of protected areas within the area under investigation was used as the last criterion. Protected Areas were avoided for dam construction, and the minimum distance between the boundary of the protected area to the dam site was at least 10 km.

3.2.3. Calculating the Dam Volume

After finalizing the exact locations for dam constructions, the volume capacity for each site was calculated at different plane heights using the surface volume tool of the functional surface toolset of the 3D analyst toolbox. We present the results and discussion first, followed by the conclusion section.

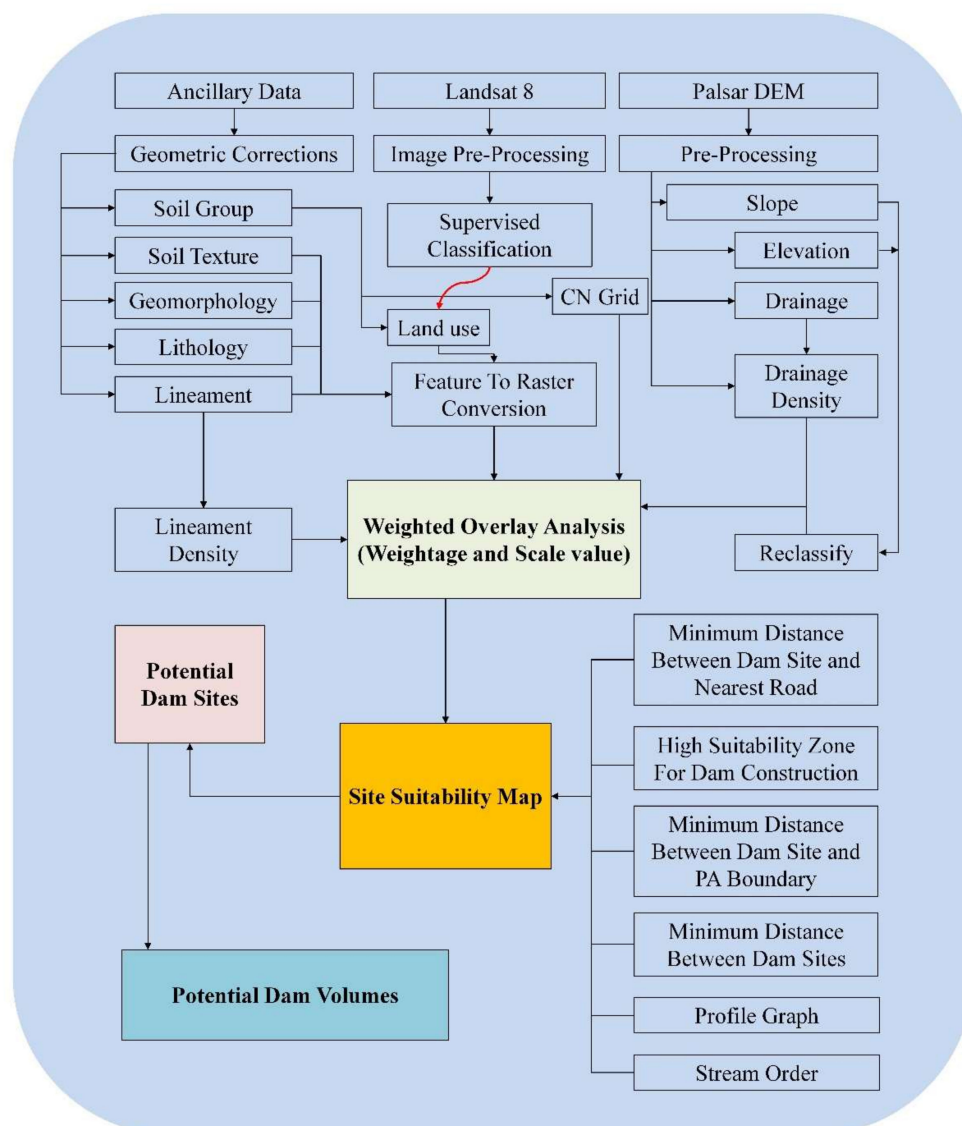


Figure 2. Overall methodology of the work shown using a hierarchy chart.

4. Results and Discussion

4.1. Parameter Weightages and Scale Values for MCA

As outlined in the methodology section, the most critical suitability factors used here are land use, lithology, geomorphology, slope, elevation, drainage density, CN grid, lineament density, soil texture.

The physical cover of the earth's surface refers to land cover (LC), and usable and usage by human beings refers to land use (LU) [56,57]. For dam site suitability analysis, LULC categories are one of the main parameters. Forest, agriculture cropland, agriculture plantation, built-up, scrub, pastures, wasteland, snow glacial, and water bodies are the different LULC classes identified in this study area (Figure 3a). The LULC category is prone to soil erosion is least favorable, since it makes a weak foundation for constructing a dam [53]. The maximum scale value of 9 was assigned to the scrub class (highly suitable), followed by the wasteland class of 7. The minimum scale value of 2 was assigned to agriculture cropland, which was the least suitable. LULC classes, agriculture plantation, forest, and pasture were assigned scale values of 3, 4, and 5, respectively. Water bodies, snow glacial, and built-up were masked in the analysis. Following the study, the LULC parameter was allocated a weightage of 15%. (Table 3).

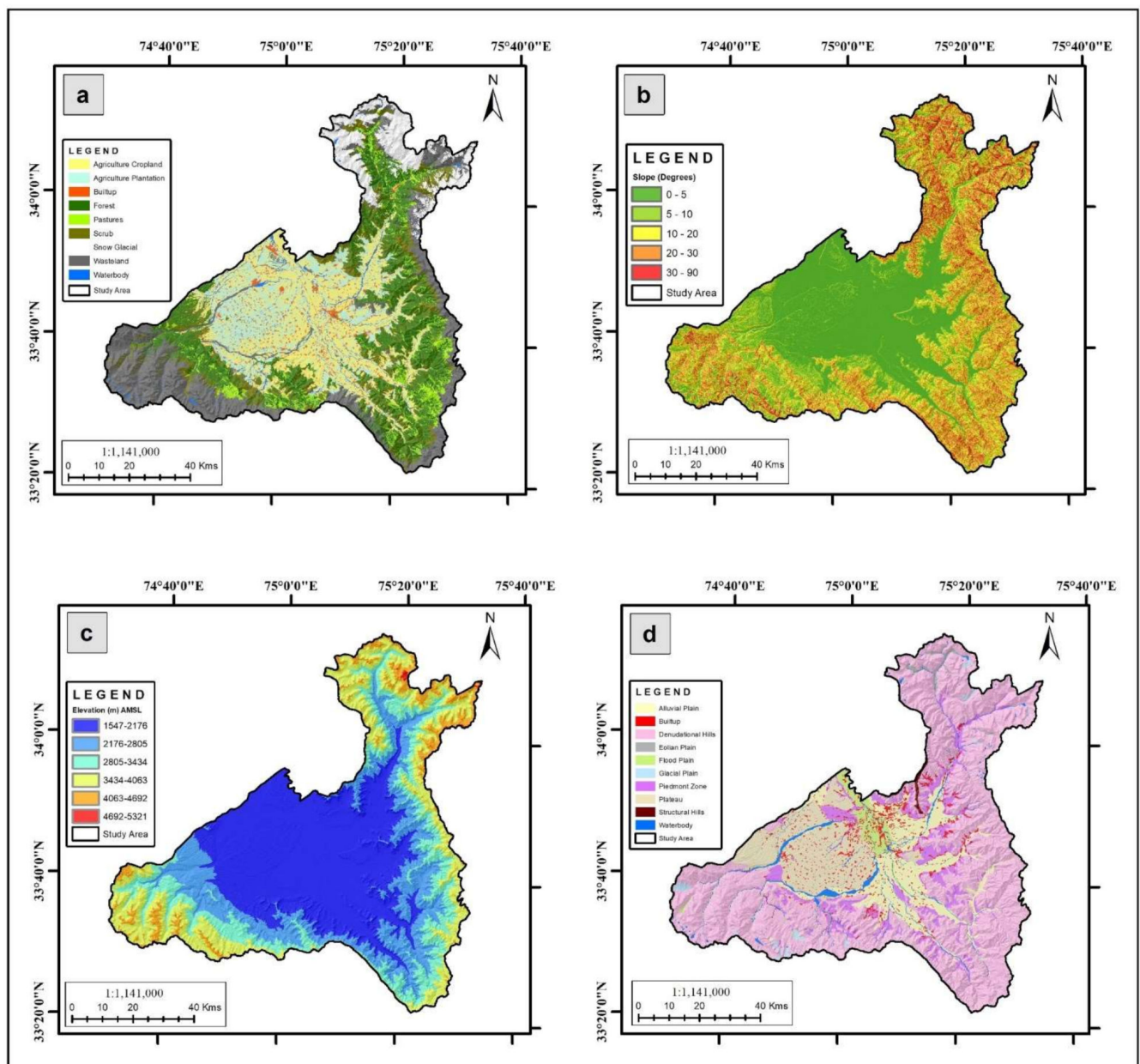


Figure 3. (a) LULC (b) Slope (c) Elevation, (d) Geomorphological classes of the study area.

The slope is the rate of change of elevation for each DEM; it is the steepness of terrain [54]. The slope value may be either in degrees (values from 0–90) or the increase in percent (percentage values range from 0 to infinity). Higher slope values indicate steep terrain [55]. Slope impacts the dam’s stability since higher slopes are more vulnerable to landslides, rendering them the least suitable location for dam construction. Higher slopes are more prone to soil erosion and involve massive earthworks [58]. The following five slope range classes were used in the present study 0–5° (Flat), 5–10° (Gentle), 10–20° (Medium slope), 20–30° (Steep slopes), and 30–90° (Very Steep slopes) (Figure 3b). The overall weight of the slope parameter in the present analysis was assigned 10%. The highest scale value, 7, was assigned to the (0–5°) slope class with high suitability for dam construction, and the lowest scale value, 1, was assigned to the (30–90°) slope class with least suitability. A scale value of 5, 3 and 2 was assigned to (5–10°), (10–20°), and (20–30°) slope classes, respectively. The slope parameter was assigned a weightage of 10% overall (Table 3).

Table 3. Weightage and scale values for different thematic layers and their classes, respectively.

S. No	Layers	Classes	Weights	Scale Value	Site Suitability
1	LULC	Agriculture Cropland	15%	2	Low
		Agriculture Plantation		3	Low
		Built-up		3	Low
		Scrub		9	High
		Forest		4	Medium
		Pasture		5	Medium
		Wasteland		7	High
		Water		Restricted	Nil
2	Slope (degrees)	Snow Glacial	10%	Restricted	Nil
		0–5		7	High
		5–10		5	Medium
		10–20		3	Low
		20–30		2	Low
3	Elevation (m)	30–90	10%	1	Low
		1547–2176		9	High
		2176–2805		7	High
		2805–3434		5	Medium
		3434–4063		3	Low
		4063–4692		2	Low
4	Geomorphology	4692–5321	15%	1	Low
		Alluvial plain		9	High
		Flood plain		9	High
		Eolian plain		2	Low
		Glacial plain		Restricted	Nil
		Piedmont zone		8	High
		Plateau		4	Medium
Denudational hill	1	Low			
5	Lithology	Structural hills	10%	1	Low
		Amygdaloidal Basalt		9	High
		Bedded Limestone		3	Low
		Phyllite Schist Slate Quartzite Bed		5	Medium
		Phyllite Schist Slate Bed		2	Low
		Quartzite Shale Phyllite Bed		8	High
		Sandstone Claystone Siltstone Bed		4	Medium
6	Lineament Density	Alluvium	10%	1	Low
		0–0.31		9	High
		0.31–0.62		7	High
		0.62–0.93		5	Medium
		0.93–1.24		2	Low
7	Drainage Density	1.24–1.55	10%	1	Low
		0.17–0.8		1	Low
		0.81–1.1		2	Low
		1.2–1.4		4	Medium
		1.5–1.8		8	High
8	CN Grid Value	1.9–2.4	10%	9	High
		30–48		1	Low
		49–67		3	Low
		68–78		5	Medium
		79–85		7	High
86–100	9	High			

Table 3. Cont.

S. No	Layers	Classes	Weights	Scale Value	Site Suitability
9	Soil Texture	Clay	10%	9	High
		Sand		1	Low
		Silt		1	Low
		Loam		8	High
		Clay Loam		7	High
		Sandy Clay Loam		6	Medium
		Sandy Loam		2	Low
		Silt Loam		3	Low
		Silty Clay		4	Medium
		Silty Clay Loam		5	Medium
Rock Outcrop	Restricted	Nil			

Elevation of the location is the height above mean sea level, affecting the accumulation and flow of water [58]. Low-level regions are more suited for dam building since the danger of water storage is smaller, and groundwater is more suitable at a lower elevation [48]. The present study area is divided into six elevation zones (Figure 3c), and lower elevation ranges were assigned large-scale values and vice versa. The highest scale value of 9 was given to the lowest elevation range (1547–2176 m) as this elevation range is highly suitable for dam construction, followed by 7 to range (2176–2805 m). The least scale value of 1 was given to the highest elevation range (4692–5321 m) as this elevation range is least suitable for dam construction. A scale value of 2, 3, and 5 were assigned to range (4063–4692 m), range (3434–4063 m), and range (2805–3434 m), respectively. Furthermore, the overall weightage provided to the elevation parameter was 10% (Table 3).

Geomorphology is the study of origin, evolution, and processes of formation of land-forms. Areas occupied by flood plains, alluvial plains, river valleys, and piedmont zones are more suitable for dam construction. The runoff speed is low, and water trapping is a lot easier than in areas occupied by hills and mountains [59]. The different geomorphological classes identified in the study area are alluvial plain, flood plain, eolian plain, glacial plain, piedmont zone, plateau, denudational hill, and structural hills (Figure 3d). The highest scale values of 9 were given to alluvial and flood plain classes, followed by 8 to piedmont zone, as these geomorphological classes are highly suitable for dam construction. The least scale value of 1 was given to denudational hill, structural hill, and glacial plain being the least ideal for dam construction. Plateau and eolian plain geomorphological classes were assigned scale values of 4 and 2, respectively. An overall weightage of 15% was given the said parameter (Table 3).

Lithology studies rocks, including their color, composition, texture, and formation. Rocks in which grain to grain contact are strong, like massive igneous rocks and deformation-free metamorphic rocks, form a strong foundation and support the least infiltration of water (leakage) for dam construction to the sedimentary rock where grain to grain contact is weak [60]. In the present study, different lithological units identified were amygdaloidal basalt, bedded limestone, phyllite schist slate quartzite bed, phyllite schist slate bed, quartzite shale phyllite bed, sandstone claystone siltstone bed, and alluvium (Figure 4a).

The highest scale value of 9 was given to amygdaloidal basalt followed by 8 to quartzite shale phyllite bed as these lithological units are highly suitable for dam construction. The least scale value of 1 was given to alluvium, being the least ideal for dam construction. Phyllite schist slate quartzite bed, Sandstone claystone siltstone bed, bedded limestone, and phyllite schist slate bed lithological units were given scale values of 5, 4, 3, and 2, respectively. This parameter was given an overall weightage of 10% (Table 3).

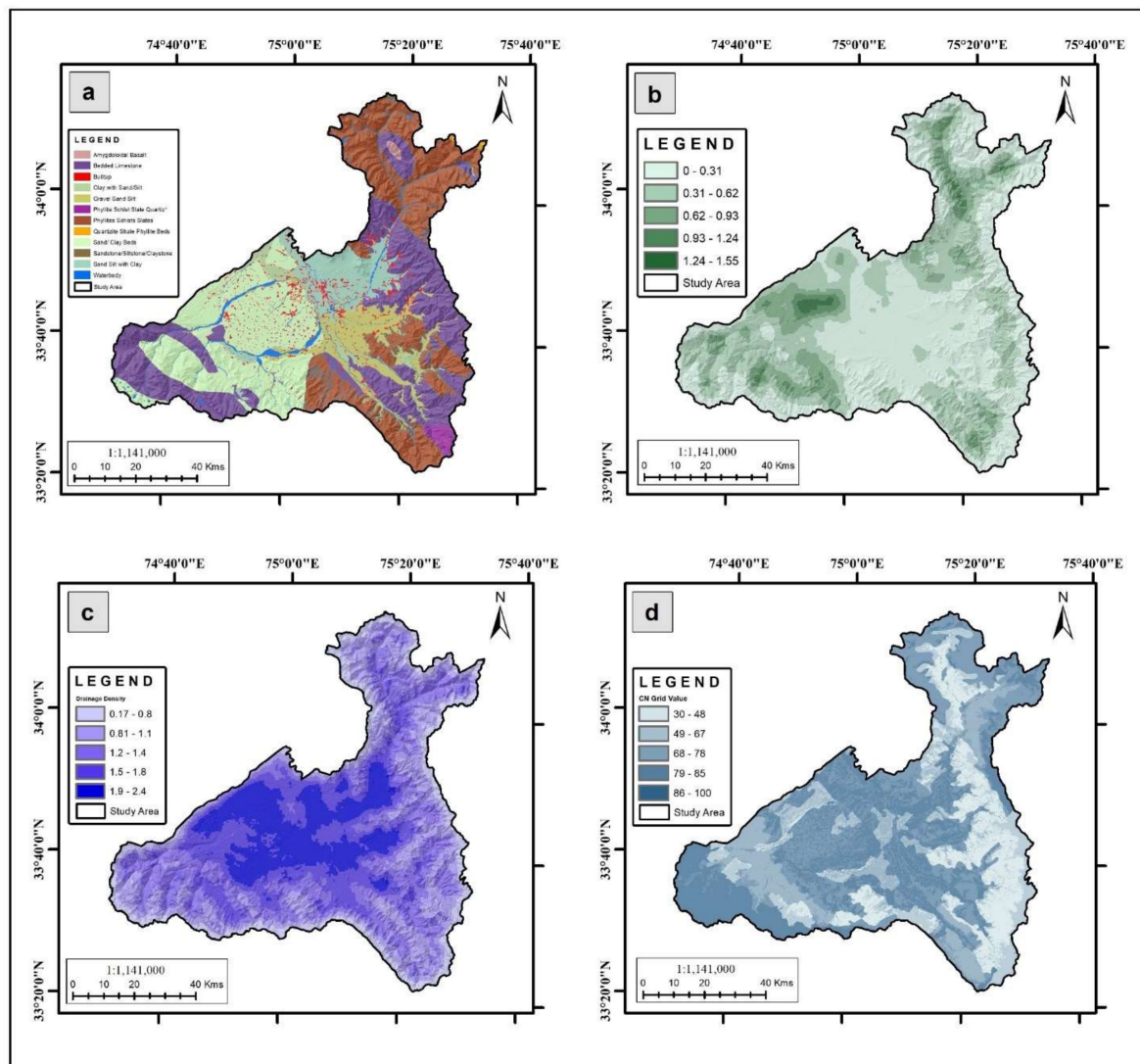


Figure 4. (a) Lithology (b) Lineament (c) Drainage density (d) CN Grid of the study area.

A lineament represents a linear feature in a landscape that represents underlying geological structures like fault, fracture, or joint. Lineament mapping is an essential task for oil and water exploration, landslides, and suitability studies [61]. Building any dam on geological structures like faults can prove costly as a dam can fail due to movement along the fault. Areas with high lineament density make the least suitable site for dam construction and should be avoided. The following lineament density classes were generated in the present study 0–0.31, 0.31–0.62, 0.62–0.93, 0.93–1.24 and 1.24–1.55 (Figure 4b). The least scale value of 1 was given to the 1.24–1.55 lineament density class being least suitable for dam construction. The highest scale value of 9 was given to the 0–0.31 lineament density class. Scale values of 7, 5 and 2 were given to 0.31–0.62, 0.62–0.93, 0.93–1.24, respectively. This parameter was given an overall weightage of 10% (Table 3).

The ratio of total stream length to the watershed area is known as drainage density. Areas with higher drainage density values indicate more runoff, less infiltration, and impermeable subsurface [50], which makes a highly suitable site for dam construction. In contrast, areas with lower drainage density values indicate less runoff, more infiltration, and permeable subsurface, making it the least suitable site for dam construction (Figure 4c). In the present study, the areas with a higher drainage density value of 1.9–2.4 were given a scale value of 9, followed by a scale value of 8 assigned to a drainage density class of 1.5–1.8. The least scale value of 1 was given to the drainage density class of 0.17–0.8. The drainage

density classes 0.81–1.1 and 1.2–1.4 were given 2 and 4, respectively. This parameter was given an overall weightage of 10% (Table 3).

Curve Number is one of the essential methods of computing runoff. The values of CN range from 30 to 100. Higher CN values indicate more runoff and less infiltration and whereas lower CN values indicate less runoff and more infiltration [62]. Areas with higher CN value make a good suitability site for dam construction. In the present study, five classes of CN grid values were generated (Figure 4d). The highest scale value of 9 was given to the class, 86–100, whereas the least scale value of 1 was given to the 30–48. Scale values of 7, 5, and 3 were given to 79–85, 68–78, and 49–67, respectively; it was given an overall weightage of 10% (Table 3).

Soil texture is the comparative proportion of sand, silt, and clay in the soil. The rates of runoff and infiltration are both affected by soil texture. Soils with good water holding volumes are more suitable for dam construction. Due to higher water retention, fine and medium-textured soils are more required for dam construction [63]. The different soil texture classes identified in the study area are clay, sand, silt, loam, clay loam, sandy clay loam, sandy loam, silt loam, silty clay, silty clay loam, and rock outcrop (Figure 5a); moreover, the soil texture map was used to create a soil group map (Table 3, Figure 5b). The stream order map is shown in Figure 5c.

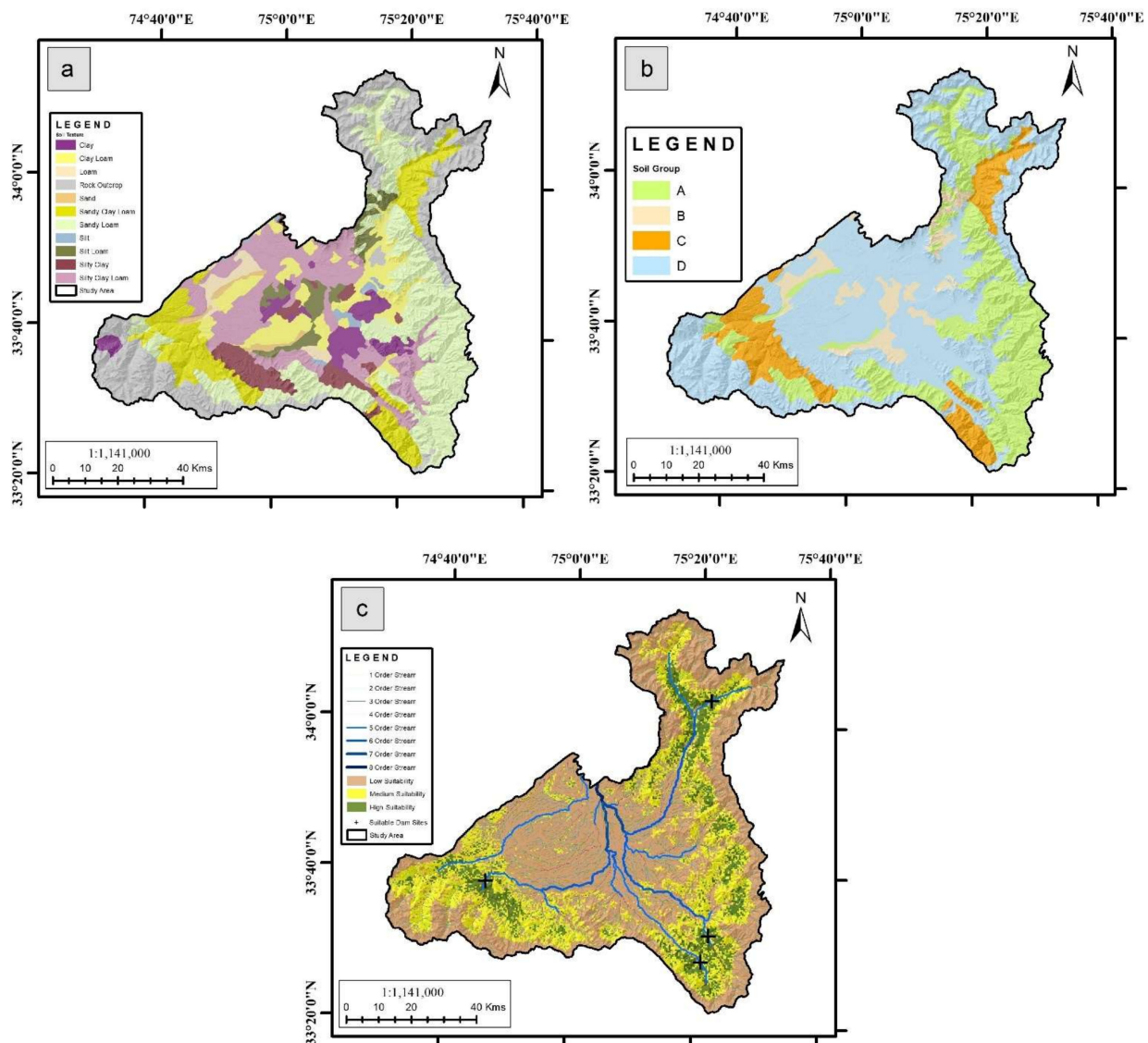


Figure 5. (a) Soil texture; (b) Soil group; (c) Stream order maps of the study area.

The highest scale value of 9 was given to clay for the soil texture layer, followed by 8 to loam. The least scale value of 1 was given to soil texture classes of sand and silt. The other soil texture classes, clay loam, sandy clay loam, silty clay loam, silty clay, silty loam, and sandy loam, were given scale values of 7, 6, 5, 4, 3, and 2, respectively; it was given an overall weightage of 10%.

4.2. Suitable Dam Sites

The results of the MCA revealed that out of the total (4347.74 km²) area evaluated for the dam suitability, 477.74 km² (10.98%) of the area falls in the high suitability zone, 1255.73 km² (28.88%) of the area falls in medium suitability zone, whereas 2614.66 km² (60.14%) of the area falls in low suitability zone (Figure 6).

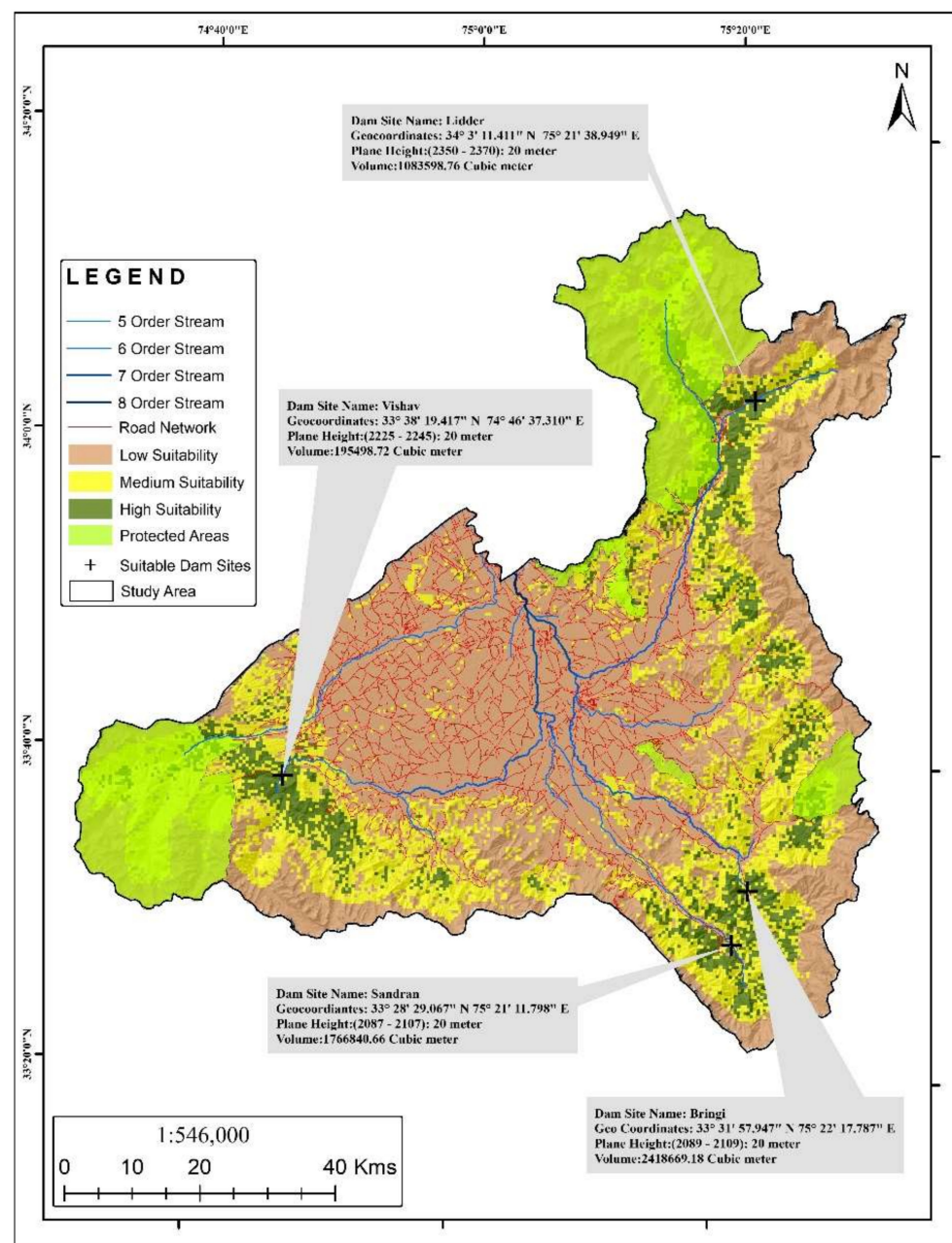


Figure 6. Suitable site for dam construction.

Further, as described in the methodology section, the final mapping of the exact location involved the knowledge-driven assessment based on six criteria: stream order, suitability zone, minimum dam site interval, distance from roads to the dam site, distance from protected areas dam site- and topography. Based on these criteria, a total of four suitable sites were identified (Figure 6). Out of the six watersheds Lidder, Kuthar, Bringi, Sandran, Vishav, and Rembiara of the present study, a single suitable site for dam construction was identified for each of the four watersheds Lidder, Bringi, Sandran, and Vishav, whereas no suitable site for dam construction was identified for Kuthar and Rembiara watersheds. The Kuthar and Rembiara watersheds are considered unsuitable for constructing any dam as the watersheds did not satisfy all the six criteria considered from site suitable site for dam construction. The elevation profiles of the four selected dam sites are shown in Figure 7.

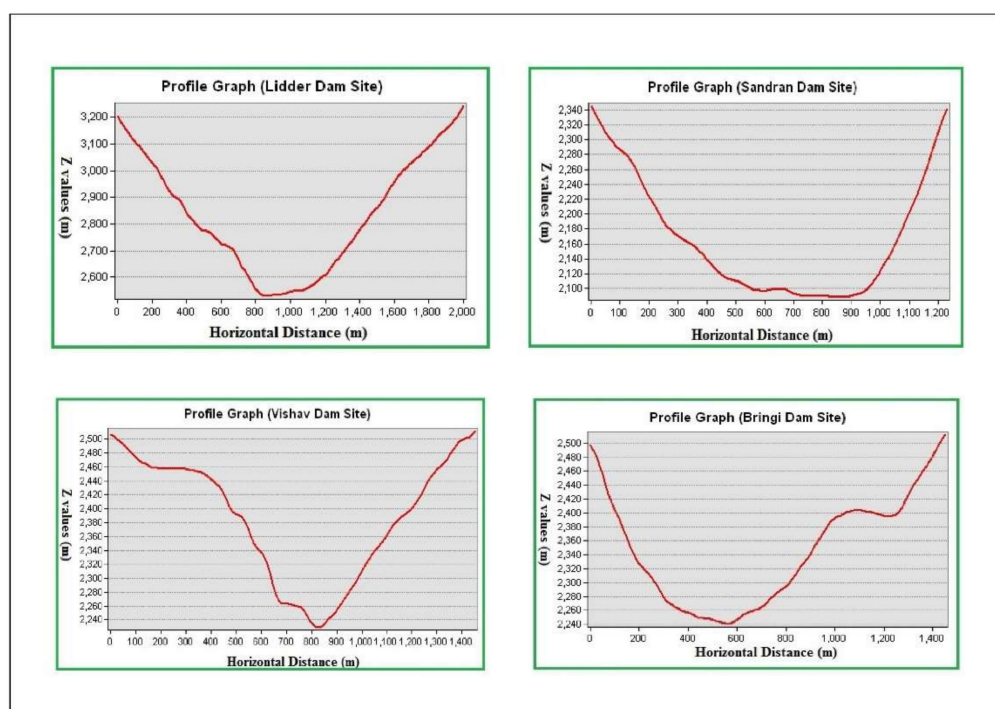


Figure 7. Profile graphs of the selected dam sites.

4.3. Volumes of the Dam Sites

For 20 m of height from the base height value, the total volume calculated for the Bringi, Lidder, Sandran, and Vishav is $2,418,669.18 \text{ m}^3$, $1,083,598.76 \text{ m}^3$, $1,766,840.66 \text{ m}^3$, and $195,498.72 \text{ m}^3$, respectively (Figure 6). The volume calculated at different plane heights for four suitable dam sites is given in below (Table 4).

The Bringi suitable dam site holds the highest volume of water, $2,418,669.18 \text{ m}^3$ at a plane height of 2089–2109 m, followed by sandran dam site $1,766,840.66 \text{ m}^3$ at a plane height of 2087–2107 m and Vishav dam site $195,498.72.66 \text{ m}^3$ at a plane height of 2225–2245. The Lidder suitable dam site holds the least volume of water, $1,083,598.76 \text{ m}^3$ at a plane height of 2350–2370 m. The geo-coordinates of the suitable dam construction sites are listed below in Table 5.

Besides flood mitigation, the proposed dams would be applicable as water reservoirs during periods of water scarcity, and they can be used for agriculture, drinking, and other uses. The planned dam locations are one of several potential answers to the region's water constraint. The proposed dam locations might be utilized to gather water from watersheds and artificially recharge groundwater. These dams can also be a significant source of hydropower generation. Various studies have been conducted for the determination of potential dam sites using the MCA approach. Shao et al. (2020) conducted a MCA to identify the potential dam construction sites in the Panjkora river basin, Pakistan. The

study used stream order, geology, and LULC information to map the potential dam sites using a weighted overlay analysis approach. Their weightage and scaling values were similar to the present study. The study aimed to map such locations for flood disaster risk management and water storage [52]. Hashim and Sayl (2021) used various parameters for locating the sites for rainwater harvesting in Iraq using Boolean overlay analysis technique. The authors used LULC topography, road information for conducting this study [64]. Similarly, there have been various conducted recently for finding the appropriate sites for dam construction such as Adham et al. (2018), Mugo and Odera (2019), Othman et al. (2020), Sayl et al. (2020), Alam et al. (2021), Aly et al. (2022) among various others [65–70].

It must be noted that all these sites were determined using the most appropriate parameters, their weightage, and the scaling values; however, these are proposed sites only, and the authorities need to conduct field-based assessment studies further to find the best site for dam construction. This study helped narrow down the most suitable area for dam construction in the south Kashmir valley.

Table 4. Volume calculation at different plane heights for proposed dam sites.

Watershed-Wise Dam Site Location	Elevation Range (m)	Plane Height (m)	Volume (m ³)
Bringi	2089–4339	2089	0
		2094	87,557.12
		2099	485,274.20
		2104	1,240,961.47
		2109	2,418,669.18
Lidder	2350–5321	2350	0
		2355	6703.41
		2360	34,827.21
		2365	336,015.74
		2370	1,083,598.76
Sandran	2087–4091	2087	0
		2092	21,015.63
		2097	216,953.70
		2102	800,106.73
		2107	1,766,840.66
Vishav	2225–4614	2225	0
		2230	5943.94
		2235	34,418.50
		2240	95,838.34
		2245	195,498.72

Table 5. Geo-coordinates of proposed dam sites.

S. No	Site Name	Elevation (m)	Latitude	Longitude
1	Bringi	2195	33°30′48.82″N	75°22′55.40″E
2	Lidder	2350	34°3′11.411″N	75°21′38.949″E
3	Sandran	2087	33°28′29.067″N	75°21′11.798″E
4	Vishav	2225	33°38′19.417″N	74°46′37.310″E

4.4. Validation and Open-and-Shut Mechanism for Flood Management

It must be noted that the proposed dams for flood management in this study shall act as reservoirs during extensive precipitation events that might trigger flood deluge in the downstream areas, either larger or smaller in magnitude than the great-2014 flood in the Kashmir valley. The 2014 floods in the Kashmir valley have been extensively studied, and it has been declared as a 50-year flood [25]. Figure 8 shows the extreme discharge at the Sangam station during this event. It can be observed that the event was an extreme event not seen in the last five decades.

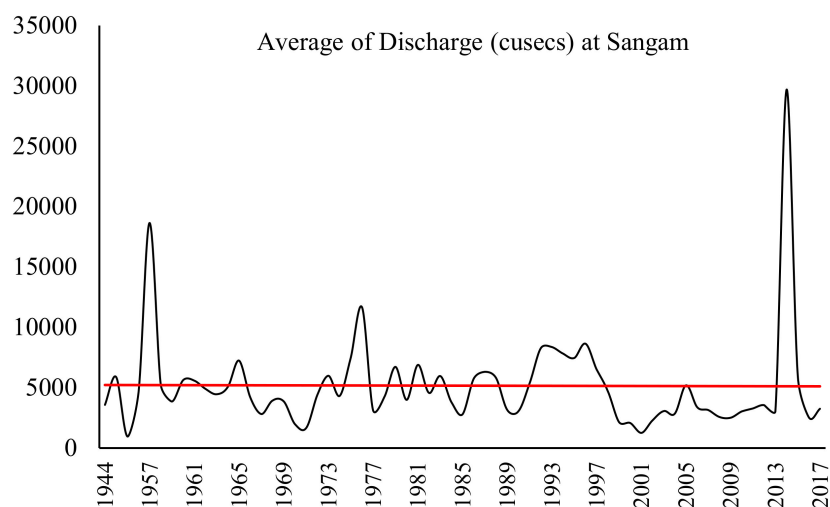


Figure 8. Annual average discharge at Sangam (Source: I&FC, Department).

To understand the efficiency of proposed dams and the amount of water they can retain, we have compared the proposed dam volumes with the volume of water generated in a single day during the 2014 floods. Table 6 shows the volume of water generated on the given dates during the 2014 floods in the Kashmir valley. The valley-wide storm precipitation event lasted between 6 September to 11 September 2014. On 9 September 2014, almost the whole valley was inundated. Here, we propose a scenario that if the same magnitude of flood occurs again, and if the proposed dam structure is in place, then according to the estimates presented in Table 6, the dam at Lidder (Sheeshnag) would retain 15.15% of the volume of water generated. Similarly, the proposed dams at Bringi, Sandran, and Vishaw would retain 55.36%, 6.85%, and 0.26% of the generated volume. It is notable to mention here that this massive volume of the retained water will provide the flood management authorities ample time to plan for efficient mechanisms to avoid a disaster-like scenario, as was witnessed during the 2014 deluge.

Table 6. The volume of water generated at different dates during the 2014-flood deluge of Kashmir valley and the volume of the proposed dams.

Dam Location	Date	Volume of Water Generated * (Megalitres, 10 ⁶)	Capacity of Proposed Dam (Megalitres, 10 ⁶)	Percent Retained (%)
Lidder at Sheshnag	06-09-2014	7154.58	1083.6	15.15
Bringi	06-09-2014	4368.76	2418.67	55.36
Sandran	07-09-2014	25,789.78	1766.84	6.85
Vishaw	08-09-2014	74,809.93	195.5	0.26

* Volume estimates generated from discharge data provided by the Irrigation and Flood Control Department, Government of Jammu and Kashmir.

One of the critical reasons for failed flood management during the 2014 floods was the sudden surge of the water at the intersection of the south Kashmir watersheds, particularly at the *Sangam* location (confluence of Kuthar, Lidder, Sandran, Vishaw streams) [38]. This extreme surge of water triggered bund breaches along the Jhelum river, particularly in central Kashmir (Srinagar and Pampore), resulting in a widespread disaster; these proposed dams shall serve as points of control to restrict such a surge to help in early warning, evacuation, and infrastructural measures in case of floods. We refer to this mechanism as the open-and-shut mechanism of flood management. By alternate closing and opening, the barrages of these dams using a well-calculated strategy, the sudden surge at the confluence of these streams can be minimized to a large extent and help provide ample time for flood management downstream.

This analysis, however, has limitations regarding the mismatch of discharge and the dam sites; however, here, an understanding of the operating mechanism of flood control dam infrastructure is presented. Such uncertainty due to location mismatch is manageable when the usefulness of such an infrastructure is scientifically established; further, the present work is aimed to propose the dam sites and show their effectiveness. The relevant authorities shall have to further investigate and validate the proposed dam sites using ground-based engineering surveys and decide on the construction of dam sites accordingly.

We did not consider the dam sites within the protected areas due to legal and conservation issues in the present analysis. This is the reason that although west Lidder would contribute more streamflow and our analysis also had shown a dam site within it, we did not propose it in the results because it harbors the Overa-Aru Wildlife sanctuary. It is believed that this work shall contribute significantly to the holistic management of the floods in the Jhelum basin.

5. Conclusions

Identifying appropriate dam construction sites is a critical planned initiative for storing and retaining enormous quantities of water for hydropower, irrigation, human consumption, industrial purposes, besides being a necessary means of flood control. In this study, the integration of all the layers (i.e., LULC, slope, elevation, geomorphology, lithology, lineament density, CN grid, and soil) governing the hydrological control over a watershed helped identify areas suitable for dam construction. Accordingly, the study area was categorized into three site suitability zones (highly suitable, medium suitable, and low suitable zones) to construct reservoir dams. Out of the total (4347.74 km²) area considered for the present study, 10.98% of the entire area falls within the high suitability zone, the medium suitability zone, 28.88% of the total area whereas 60.14% of the total area falls within the low suitability zone. Four suitable dam sites with a total volume holding capacity of 4,489,367.55 m³ for dam constructions were further identified. These proposed locations can be used to build dams for drinking water supplies, hydropower, and irrigation storage. Since the present study was part of the J&K Government's plan to mitigate and manage floods in the Jhelum basin through the Department of flood and irrigation, it is proposed the sites determined using this analysis shall be further verified for various engineering social, and legal aspects. Overall, the present research would enable hydrologists, decision-makers, and planners to establish plans to reduce damage caused by flooding and develop effective strategies to minimize the frequency of flood incidents.

Author Contributions: Conceptualization, M.F., M.A.R. and G.M.; methodology, M.F. and M.A.R.; software, M.F., M.A.R., B.A.S. and G.M.; validation, M.F., M.A.R., B.A.S., G.M., P.K., S.K.S. and S.K.; formal analysis M.F., M.A.R. and G.M.; investigation, M.F., M.A.R. and G.M.; resources, P.K., M.F. and N.S.; data curation, M.F. and M.A.R.; writing—original draft preparation, M.F., M.A.R. and G.M.; writing—review and editing G.M., M.F., M.A.R., P.K., S.K.S., S.P.T. and S.K.; visualization, M.F., M.A.R., B.A.S. and G.M.; supervision, M.F.; project administration, M.F., P.K., S.P.T. and N.S.; funding acquisition, P.K. All authors have read and agreed to the published version of the manuscript.

Funding: This publication is supported by the Asia Pacific Network for Global Change Research (APN) under Collaborative Regional Research Programme (CRRP) with project reference number CRRP2019-01MY-Kumar.

Institutional Review Board Statement: Not applicable.

Informed Consent Statement: Not applicable.

Data Availability Statement: Data is available on request from the corresponding authors.

Acknowledgments: The authors express gratitude to the experts of Department of Irrigation and Flood Control, Government of Jammu and Kashmir for providing the necessary information and data. We would also like to thank the Department of Wildlife, Government of Jammu and Kashmir for supporting us during the mapping of the protected areas. The author G.M. is thankful to the Department of Science and Technology, Government of India, for providing the Fellowship under

Scheme for Young Scientists and Technology (SYST-SEED) [Grant no. SP/YO/2019/1362(G) & (C)]. Finally, we would like to thank all the four anonymous reviewers who, through their critical analysis of our work, helped us improve this manuscript.

Conflicts of Interest: The authors declare no conflict of interest.

References

- Letcher, T. *The Impacts of Climate Change: A Comprehensive Study of Physical, Biophysical, Social, and Political Issues*; Elsevier: Amsterdam, The Netherlands, 2021.
- Kaltenborn, B.P.; Nellesmann, C.; Vistnes, I.I. *High Mountain Glaciers and Climate Change: Challenges to Human Livelihoods and Adaptation*; UNEP, GRID: Arendal, Norway, 2010.
- Lala, J.M.; Rounce, D.R.; McKinney, D.C. Modeling the glacial lake outburst flood process chain in the Nepal Himalaya: Reassessing Imja Tsho's hazard. *Hydrol. Earth Syst. Sci.* **2018**, *22*, 3721–3737. [[CrossRef](#)]
- Youssef, A.M.; Abu-Abdullah, M.M.; AlFadail, E.A.; Skilodimou, H.D.; Bathrellos, G.D. The devastating flood in the arid region a consequence of rainfall and dam failure: Case study, Al-Lith flood on 23th November 2018, Kingdom of Saudi Arabia. *Z. Für Geomorphol.* **2021**, *63*, 115–136. [[CrossRef](#)]
- Youssef, A.M.; Al-Harbi, H.M.; Zabramwi, Y.A.; El-Haddad, B.A. *Human-Induced Geo-Hazards in the Kingdom of Saudi Arabia: Distribution, Investigation, Causes and Impacts. Geohazards Caused by Human Activity*; Farid, A., Ed.; InTech: Horwich, UK, 2016; pp. 37–61.
- Dunn, R.J.; Stanitski, D.M.; Gobron, N.; Willett, K.M.; Ades, M.; Adler, R.; Allan, R.; Allan, R.P.; Anderson, J.; Argüez, A.; et al. Global climate. *Bull. Am. Meteorol. Soc.* **2020**, *101*, S9–S127. [[CrossRef](#)]
- Callaghan, T.V.; Jonasson, S. Arctic terrestrial ecosystems and environmental change. In *The Arctic and Environmental Change*; CRC Press: Boca Raton, FL, USA, 2019; pp. 59–76.
- Kanga, S.; Meraj, G.; Farooq, M.; Singh, S.K.; Nathawat, M.S. *Disaster Management in the Complex Himalayan Terrains*; Springer: Cham, Switzerland, 2022.
- Ali, N.; Alam, A.; Bhat, M.S.; Shah, B. Developing a Hazard Profile of the Kashmir Valley Through Historical Data Analysis for The Period 1900–2020. *Nat. Hazards* **2021**.
- Tomar, P.; Singh, S.K.; Kanga, S.; Meraj, G.; Kranjčić, N.; Đurin, B.; Pattanaik, A. GIS-Based Urban Flood Risk Assessment and Management—A Case Study of Delhi National Capital Territory (NCT), India. *Sustainability* **2021**, *13*, 12850. [[CrossRef](#)]
- Akbulut, N.E.; Bayarı, S.; Akbulut, A.; Özyurt, N.N.; Sahin, Y. Rivers of Turkey. In *Rivers of Europe*; Elsevier: Amsterdam, The Netherlands, 2022; pp. 851–880.
- Rafiq, M.; Meraj, G.; Kesarkar, A.P.; Farooq, M.; Singh, S.K.; Kanga, S. Hazard Mitigation and Climate Change in the Himalayas—Policy and Decision Making. In *Disaster Management in the Complex Himalayan Terrains*; Springer: Cham, Switzerland, 2022; pp. 169–182.
- Flash Floods in Uttarakhand, Himachal Pradesh; Over 30 Feared Dead. IBNLive. 5 August 2012. Available online: <https://web.archive.org/web/20120806080410/http://ibnlive.in.com/news/flash-floods-hit-uttarakhand-hp-jk-30-dead/278619-3-245.html> (accessed on 2 January 2022).
- Shugar, D.H.; Jacquemart, M.; Shean, D.; Bhushan, S.; Upadhyay, K.; Sattar, A.; Schwanghart, W.; McBride, S.; de Vries, M.V.W.; Mergili, M.; et al. A massive rock and ice avalanche caused the 2021 disaster at Chamoli, Indian Himalaya. *Science* **2021**, *373*, 300–306. [[CrossRef](#)] [[PubMed](#)]
- Gobiet, A.; Kotlarski, S.; Beniston, M.; Heinrich, G.; Rajczak, J.; Stoffel, M. 21st century climate change in the European Alps—A review. *Sci. Total Environ.* **2014**, *493*, 1138–1151. [[CrossRef](#)] [[PubMed](#)]
- Europe Floods: At Least 120 Dead and Hundreds Unaccounted For. Available online: <https://www.bbc.com/news/world-europe-57858829> (accessed on 2 January 2022).
- Meraj, G.; Romshoo, S.A.; Yousuf, A.R.; Altaf, S.; Altaf, F. Assessing the influence of watershed characteristics on the flood vulnerability of Jhelum basin in Kashmir Himalaya: Reply to comment by Shah 2015. *Nat. Hazards* **2015**, *78*, 1–5. [[CrossRef](#)]
- Romshoo, S.A.; Bhat, S.A.; Rashid, I. Geoinformatics for assessing the morphometric control on hydrological response at watershed scale in the Upper Indus Basin. *J. Earth Syst. Sci.* **2012**, *121*, 659–686. [[CrossRef](#)]
- Bhat, M.S.; Alam, A.; Ahmad, B.; Kotlia, B.S.; Farooq, H.; Taloor, A.K.; Ahmad, S. Flood frequency analysis of river Jhelum in Kashmir basin. *Quat. Int.* **2019**, *507*, 288–294. [[CrossRef](#)]
- Alam, A.; Bhat, M.S.; Farooq, H.; Ahmad, B.; Ahmad, S.; Sheikh, A.H. Flood risk assessment of Srinagar city in Jammu and Kashmir, India. *Int. J. Disaster Resil. Built Environ.* **2018**, *9*. [[CrossRef](#)]
- Bhatt, C.M.; Rao, G.S.; Farooq, M.; Manjusree, P.; Shukla, A.; Sharma, S.V.S.P.; Kulkarni, S.S.; Begum, A.; Bhanumurthy, V.; Diwakar, P.G.; et al. Satellite-based assessment of the catastrophic Jhelum floods of September 2014, Jammu & Kashmir, India. *Geomat. Nat. Hazards Risk* **2017**, *8*, 309–327.
- Rather, M.A.; Farooq, M. Remote Sensing & GIS for the Assessment of Flood Affected Population. A Case Study of September 2014 Floods in Kashmir J&K India. *Int. J. Eng. Res.* **2018**, *7*, 35–37.
- Malik, I.H. Spatial dimension of impact, relief, and rescue of the 2014 flood in Kashmir Valley. *Nat. Hazards* **2021**, 1–19. [[CrossRef](#)]

24. Meraj, G.; Romshoo, S.A.; Yousuf, A.R.; Altaf, S.; Altaf, F. Assessing the influence of watershed characteristics on the flood vulnerability of Jhelum basin in Kashmir Himalaya. *Nat. Hazards* **2015**, *77*, 153–175. [[CrossRef](#)]
25. Romshoo, S.A.; Altaf, S.; Rashid, I.; Dar, R.A. Climatic, geomorphic and anthropogenic drivers of the 2014 extreme flooding in the Jhelum basin of Kashmir, India. *Geomat. Nat. Hazards Risk* **2018**, *9*, 224–248. [[CrossRef](#)]
26. Meraj, G.; Khan, T.; Romshoo, S.A.; Farooq, M.; Rohitashw, K.; Sheikh, B.A. An integrated geoinformatics and hydrological modelling-based approach for effective flood management in the Jhelum Basin, NW Himalaya. *Proceedings* **2018**, *7*, 8. [[CrossRef](#)]
27. Abu-Abdullah, M.M.; Youssef, A.M.; Maerz, N.H.; Abu-AlFadail, E.; Al-Harbi, H.M.; Al-Saadi, N.S. A flood risk management program of Wadi Baysh dam on the downstream area: An integration of hydrologic and hydraulic models, Jizan region, KSA. *Sustainability* **2020**, *12*, 1069. [[CrossRef](#)]
28. Mei, X.; Van Gelder, P.H.A.J.M.; Dai, Z.; Tang, Z. Impact of dams on flood occurrence of selected rivers in the United States. *Front. Earth Sci.* **2017**, *11*, 268–282. [[CrossRef](#)]
29. Peyravi, M.; Peyvandi, A.A.; Khodadadi, A.; Marzaleh, M.A. Flood in the South-West of Iran in 2019; causes, problems, actions and lesson learned. *Bull. Emerg. Trauma* **2019**, *7*, 199. [[CrossRef](#)]
30. Rokaya, P.; Wheeler, H.; Lindenschmidt, K.E. Promoting sustainable ice-jam flood management along the Peace River and Peace-Athabasca Delta. *J. Water Resour. Plan. Manag.* **2019**, *145*, 04018085. [[CrossRef](#)]
31. Smys, S.; Basar, A.; Wang, H. CNN based flood management system with IoT sensors and cloud data. *J. Artif. Intell.* **2020**, *2*, 194–200.
32. Mohanty, M.P.; Mudgil, S.; Karmakar, S. Flood management in India: A focussed review on the current status and future challenges. *Int. J. Disaster Risk Reduct.* **2020**, *49*, 101660. [[CrossRef](#)]
33. Best, J. Anthropogenic stresses on the World's big rivers. *Nat. Geosci.* **2019**, *12*, 7–21. [[CrossRef](#)]
34. Hornberger, G.M.; Perrone, D. *Water Resources: Science and Society*; Johns Hopkins University Press: Baltimore, MA, USA, 2019.
35. Smith, L.C. *Rivers of Power: How a Natural Force Raised Kingdoms, Destroyed Civilizations, and Shapes Our World*; Penguin: London, UK, 2020.
36. Singh, R.; Patel, S.K.; Tiwari, A.K.; Singh, G.S. Assessment of flood recession farming for livelihood provision, food security and environmental sustainability in the Ganga River Basin. *Curr. Res. Environ. Sustain.* **2021**, *3*, 100038. [[CrossRef](#)]
37. Kalambukattu, J.; Kumar, S. Modelling soil erosion risk in a mountainous watershed of Mid-Himalaya by integrating RUSLE model with GIS. *Eurasian J. Soil Sci.* **2017**, *6*, 92–105. [[CrossRef](#)]
38. Pokhrel, Y.; Burbano, M.; Roush, J.; Kang, H.; Sridhar, V.; Hyndman, D.W. A review of the integrated effects of changing climate, land use, and dams on Mekong river hydrology. *Water* **2018**, *10*, 266. [[CrossRef](#)]
39. Langat, P.K.; Kumar, L.; Koech, R. Monitoring river channel dynamics using remote sensing and GIS techniques. *Geomorphology* **2019**, *325*, 92–102. [[CrossRef](#)]
40. Kareem, H. Study of Water Resources by Using 3D Groundwater Modelling in Al-Najaf Region, Iraq. Doctoral Dissertation, Cardiff University, Wales, UK, 2018.
41. Jamali, A.A.; Randhir, T.O.; Nosrati, J. Site suitability analysis for subsurface dams using Boolean and fuzzy logic in arid watersheds. *J. Water Resour. Plan. Manag.* **2018**, *144*, 04018047. [[CrossRef](#)]
42. Noori, A.M.; Pradhan, B.; Ajaj, Q.M. Dam site suitability assessment at the Greater Zab River in northern Iraq using remote sensing data and GIS. *J. Hydrol.* **2019**, *574*, 964–979. [[CrossRef](#)]
43. Al-Ruzouq, R.; Shanableh, A.; Yilmaz, A.G.; Idris, A.; Mukherjee, S.; Khalil, M.A.; Gibril, M.B.A. Dam site suitability mapping and analysis using an integrated GIS and machine learning approach. *Water* **2019**, *11*, 1880. [[CrossRef](#)]
44. Forzieri, G.; Gardenti, M.; Caparrini, F.; Castelli, F. A methodology for the pre-selection of suitable sites for surface and underground small dams in arid areas: A case study in the region of Kidal, Mali. *Phys. Chem. Earth Parts A/B/C* **2008**, *33*, 74–85. [[CrossRef](#)]
45. Raza, M.; Ahmad, A.; Mohammad, A. *The Valley of Kashmir a Geographical Interpretations. The Land*; Vikas Publishing House: New Delhi, India, 1978; Volume 1.
46. Meraj, G.; Romshoo, S.A.; Ayoub, S.; Altaf, S. Geoinformatics-based approach for estimating the sediment yield of the mountainous watersheds in Kashmir Himalaya, India. *Geocarto Int.* **2018**, *33*, 1114–1138. [[CrossRef](#)]
47. Meraj, G.; Farooq, M.; Singh, S.K.; Islam, M.; Kanga, S. Modeling the sediment retention and ecosystem provisioning services in the Kashmir valley, India, Western Himalayas. *Model. Earth Syst. Environ.* **2021**. [[CrossRef](#)]
48. Shyam, M.; Meraj, G.; Kanga, S.; Farooq, M.; Singh, S.K.; Sahu, N.; Kumar, P. Assessing the Groundwater Reserves of the Udaipur District, Aravalli Range, India, Using Geospatial Techniques. *Water* **2022**, *14*, 648. [[CrossRef](#)]
49. Kanga, S.; Singh, S.K.; Meraj, G.; Kumar, A.; Parveen, R.; Kranjčić, N.; Đurin, B. Assessment of the Impact of Urbanization on Geoenvironmental Settings Using Geospatial Techniques: A Study of Panchkula District, Haryana. *Geographies* **2022**, *2*, 1–10. [[CrossRef](#)]
50. Altaf, F.; Meraj, G.; Romshoo, S.A. Morphometric analysis to infer hydrological behaviour of Lidder watershed, Western Himalaya, India. *Geogr. J.* **2013**, *2013*, 178021. [[CrossRef](#)]
51. Koneti, S.; Sunkara, S.L.; Roy, P.S. Hydrological modeling with respect to impact of land-use and land-cover change on the runoff dynamics in Godavari River Basin using the HEC-HMS model. *ISPRS Int. J. Geo-Inf.* **2018**, *7*, 206. [[CrossRef](#)]
52. Shao, Z.; Jahangir, Z.; Muhammad Yasir, Q.; Mahmood, S. Identification of potential sites for a multi-purpose dam using a dam suitability stream model. *Water* **2020**, *12*, 3249. [[CrossRef](#)]

53. Njiru, F.M.; Siriba, D.N. Site Selection for an Earth Dam in Mbeere North, Embu County—Kenya. *J. Geosci. Environ. Prot.* **2018**, *6*, 113–133. [[CrossRef](#)]
54. Rahman, N.; Awangku, A.; Tai, V.; Mohammad, M.; Haron, S.; Khalid, K.; Rasid, M.; Shariff, S. Site selection of water reservoir based on weighted overlay in arcgis (case study: Bachok Kelantan). *Sci. Int.* **2021**, *33*, 135–139.
55. Adham, A.; Riksen, M.; Ouessar, M.; Ritsema, C.J. A methodology to assess and evaluate rainwater harvesting techniques in (semi-) arid regions. *Water* **2016**, *8*, 198. [[CrossRef](#)]
56. Meraj, G.; Kanga, S.; Kranjčić, N.; Đurin, B.; Singh, S.K. Role of natural capital economics for sustainable management of earth resources. *Earth* **2021**, *2*, 622–634. [[CrossRef](#)]
57. Meraj, G.; Singh, S.K.; Kanga, S.; Islam, M. Modeling on comparison of ecosystem services concepts, tools, methods and their ecological-economic implications: A review. *Model. Earth Syst. Environ.* **2022**, *8*, 15–34. [[CrossRef](#)]
58. Ansari, T.; Kainthola, A.; Singh, K.H.; Singh, T.N.; Sazid, M. Geotechnical and micro-structural characteristics of phyllite derived soil; implications for slope stability, Lesser Himalaya, Uttarakhand, India. *Catena* **2021**, *196*, 104906. [[CrossRef](#)]
59. Jasrotia, A.S.; Kumar, R.; Taloor, A.K.; Saraf, A.K. Artificial recharge to groundwater using geospatial and groundwater modelling techniques in North Western Himalaya, India. *Arab. J. Geosci.* **2019**, *12*, 1–23. [[CrossRef](#)]
60. Li, Q.B.; Wang, J.Z.; Wang, G.J.; Liu, Q.L.; Yan, C.B.; Hart, M. Evaluation of lithology variations in layered red beds with depth: An example of the Yellow River Guxian Dam, NW China. *Lithosphere* **2021**, *2021*, 7866225. [[CrossRef](#)]
61. Srinivas, K.N.S.S.S.; Kishore, P.P.; Rao, D.V. The geological site characterisation of the Mandla region, Eastern Deccan volcanic province, Central India. *J. Earth Syst. Sci.* **2019**, *128*, 1–16. [[CrossRef](#)]
62. Qi, J.; Lee, S.; Zhang, X.; Yang, Q.; McCarty, G.W.; Moglen, G.E. Effects of surface runoff and infiltration partition methods on hydrological modeling: A comparison of four schemes in two watersheds in the Northeastern US. *J. Hydrol.* **2020**, *581*, 124415. [[CrossRef](#)]
63. Ibrahim, G.R.F.; Rasul, A.; Ali Hamid, A.; Ali, Z.F.; Dewana, A.A. Suitable site selection for rainwater harvesting and storage case study using Dohuk Governorate. *Water* **2019**, *11*, 864. [[CrossRef](#)]
64. Hashim, H.Q.; Sayl, K.N. Detection of suitable sites for rainwater harvesting planning in an arid region using geographic information system. *Appl. Geomat.* **2021**, *13*, 235–248. [[CrossRef](#)]
65. Adham, A.; Sayl, K.N.; Abed, R.; Abdeladhim, M.A.; Wesseling, J.G.; Riksen, M.; Fleskens, L.; Karim, U.; Ritsema, C.J. A GIS-based approach for identifying potential sites for harvesting rainwater in the Western Desert of Iraq. *Int. Soil Water Conserv. Res.* **2018**, *6*, 297–304. [[CrossRef](#)]
66. Mugo, G.M.; Odera, P.A. Site selection for rainwater harvesting structures in Kiambu County-Kenya. *Egypt. J. Remote Sens. Space Sci.* **2019**, *22*, 155–164. [[CrossRef](#)]
67. Othman, A.A.; Al-Maamar, A.F.; Al-Manmi, D.A.M.A.; Liesenberg, V.; Hasan, S.E.; Obaid, A.K.; Al-Quraishi, A.M.F. GIS-based modeling for selection of dam sites in the Kurdistan Region, Iraq. *ISPRS Int. J. Geo-Inf.* **2009**, *9*, 244. [[CrossRef](#)]
68. Sayl, K.N.; Mohammed, A.S.; Ahmed, A.D. February. GIS-based approach for rainwater harvesting site selection. *IOP Conf. Ser. Mater. Sci. Eng.* **2020**, *737*, 012246.
69. Alam, S.; Borthakur, A.; Ravi, S.; Gebremichael, M.; Mohanty, S.K. Managed aquifer recharge implementation criteria to achieve water sustainability. *Sci. Total Environ.* **2021**, *768*, 144992. [[CrossRef](#)]
70. Aly, M.M.; Refay, N.H.; Elattar, H.; Morsy, K.M.; Bandala, E.R.; Zein, S.A.; Mostafa, M.K. Ecohydrology and flood risk management under climate vulnerability in relation to the sustainable development goals (SDGs): A case study in Nagaa Mobarak Village, Egypt. *Nat. Hazards* **2022**, 1–29. [[CrossRef](#)]